



# Clinical response to Vim's thalamic stereotactic radiosurgery for essential tremor is associated with distinctive functional connectivity patterns

Constantin Tuleasca<sup>1,2,3,4</sup> · Elena Najdenovska<sup>2,4</sup> · Jean Régis<sup>5</sup> · Tatiana Witjas<sup>6</sup> · Nadine Girard<sup>7</sup> · Jérôme Champoudry<sup>5</sup> · Mohamed Faouzi<sup>8</sup> · Jean-Philippe Thiran<sup>3,4,9</sup> · Meritxell Bach Cuadra<sup>2,3,4</sup> · Marc Levivier<sup>1,4</sup> · Dimitri Van De Ville<sup>10,11</sup>

Received: 7 November 2017 / Accepted: 26 December 2017 / Published online: 15 January 2018  
© Springer-Verlag GmbH Austria, part of Springer Nature 2018

## Abstract

**Introduction** Essential tremor (ET) is the most common movement disorder. Drug-resistant ET can benefit from standard surgical stereotactic procedures (deep brain stimulation, thalamotomy) or minimally invasive high-intensity focused ultrasound (HIFU) or stereotactic radiosurgical thalamotomy (SRS-T). Resting-state fMRI (rs-fMRI) is a non-invasive imaging method acquired in absence of a task. We examined whether rs-fMRI correlates with tremor score on the treated hand (TSTH) improvement 1 year after SRS-T.

**Methods** We included 17 consecutive patients treated with left unilateral SRS-T in Marseille, France. Tremor score evaluation and rs-fMRI were acquired at baseline and 1 year after SRS-T. Resting-state data (34 scans) were analyzed without a priori hypothesis, in Lausanne, Switzerland. Based on degree of improvement in TSTH, to consider SRS-T at least as effective as medication, we separated two groups: 1,  $\leq 50\%$  ( $n = 6$ , 35.3%); 2,  $> 50\%$  ( $n = 11$ , 64.7%). They did not differ statistically by age ( $p = 0.86$ ), duration of symptoms ( $p = 0.41$ ), or lesion volume at 1 year ( $p = 0.06$ ).

**Results** We report TSTH improvement correlated with interconnectivity strength between salience network with the left claustrum and putamen, as well as between bilateral motor cortices, frontal eye fields and left cerebellum lobule VI with right visual association area (the former also with lesion volume). Longitudinal changes showed additional associations in interconnectivity strength between right dorsal attention network with ventro-lateral prefrontal cortex and a reminiscent salience network with fusiform gyrus.

---

Elena Najdenovska and Jean Régis contributed equally to this work.

**Electronic supplementary material** The online version of this article (<https://doi.org/10.1007/s00701-017-3456-x>) contains supplementary material, which is available to authorized users.

✉ Constantin Tuleasca  
constantin.tuleasca@gmail.com; dimitri.vandeville@epfl.ch

<sup>1</sup> Neurosurgery Service and Gamma Knife Center, Centre Hospitalier Universitaire Vaudois (CHUV), Rue du Bugnon 44-46, BH-08, 1011 Lausanne, Switzerland

<sup>2</sup> Medical Image Analysis Laboratory (MIAL) and Department of Radiology-Center of Biomedical Imaging (CIBM), Centre Hospitalier Universitaire Vaudois, Lausanne, Switzerland

<sup>3</sup> Signal Processing Laboratory (LTS 5), Ecole Polytechnique Fédérale de Lausanne (EPFL), Lausanne, Switzerland

<sup>4</sup> Faculty of Biology and Medicine, University of Lausanne, Lausanne, Switzerland

<sup>5</sup> Stereotactic and Functional Neurosurgery Service and Gamma Knife Unit, CHU Timone, Marseille, France

<sup>6</sup> Neurology Department, CHU Timone, Marseille, France

<sup>7</sup> Department of Diagnostic and Interventional Neuroradiology, AMU, CRMBM UMR CNRS 7339, Faculté de Médecine et APHM, Hôpital Timone, Marseille, France

<sup>8</sup> Institute of Social and Preventive Medicine, Lausanne, Switzerland

<sup>9</sup> Department of Radiology, Centre Hospitalier Universitaire Vaudois, Lausanne, Switzerland

<sup>10</sup> Faculty of Medicine, University of Geneva, Geneva, Switzerland

<sup>11</sup> Medical Image Processing Laboratory, Ecole Polytechnique Fédérale de Lausanne (EPFL), Lausanne, Switzerland

**Conclusions** Brain connectivity measured by resting-state fMRI relates to clinical response after SRS-T. Relevant networks are visual, motor, and attention. Interconnectivity between visual and motor areas is a novel finding, revealing implication in movement sensory guidance.

**Keywords** Resting-state · fMRI · Essential tremor · Ventro-intermediate nucleus · Radiosurgery · Independent component analysis · Thalamotomy

## Introduction

Essential tremor (ET) is the most common movement disorder. Cardinal feature is tremor, occurring during voluntary movements of the upper extremities, additionally affecting the trunk, head, and voice [30]. It has been hypothesized that abnormal oscillations appearing within the so-called tremor network, involving ipsilateral motor area, ventro-intermediate nucleus (Vim) and red nucleus, and contralateral cerebellum (e.g., dentate nucleus) are driving tremor, but the exact cause is still a matter of debate [31, 32].

The first-line treatment is pharmacological. If resistance/side effects to medication occur, neurosurgical intervention is considered. The target is the Vim [4, 9, 13]. Gold standard open surgical interventions are deep brain stimulation (DBS) and radiofrequency thalamotomy both immediately effective at suppressing tremor [4, 22]. Minimally invasive alternatives are high-intensity focused ultrasound (HIFU) and stereotactic radiosurgical thalamotomy (SRS-T) [29, 44]. Radiosurgery (RS), unlike open surgery, induces progressive tremor arrest (maximum delay up to 1 year later) [13, 26, 43].

Functional magnetic resonance imaging (MRI) (fMRI) is a powerful imaging technique, which can be used to study task-based or spontaneous activity. In particular, spontaneous fluctuations are informative about functional network organization, such as the motor network, as shown by early seminal work of Biswal et al. [8]. This field has great potential for clinical studies, due to minimal necessity for patient compliance and powerful new analytic tools, that can extract rich information from resting-state fMRI (rs-fMRI) [19], thus opens avenues towards imaging-based biomarkers in multiple pathologies, including ET [5, 10, 17, 20]. Functional connectivity (FC) or interconnectivity (IC) has been classically defined as the temporal correlations between spatially remote neurophysiological events, as a deviation from statistical independence across these events, in distributed neuronal groups and areas [19].

In the present study, we used rs-fMRI to non-invasively investigate the effect of SRS-T on brain networks, by using a methodology implying no a priori hypothesis, and a standard type of analysis. We carried out independent component analysis (ICA) to extract relevant networks and examine longitudinal changes in these networks that are correlated with treatment response. We expected that resting-state fMRI longitudinal changes relate to tremor arrest after SRS-T.

## Methods

### Patients

We prospectively included 17 consecutive patients (right-sided tremor, drug-resistant, fulfilling criteria, Table 1) treated only with left unilateral SRS-T in Marseille, France, between September 2014 and August 2015. This study received approval (CHU Timone, CPPRB1) from the Ethical Committee of the Marseille University Hospital. Written informed consent was obtained from all patients (inclusion criteria, Table 1). All cases were referred by a movement disorders neurologist (TW).

Baseline tremor (by TW) and neuroimaging assessment (on a single 3-T MR machine, Siemens Skyra, Munich, Germany, T1, and rs-fMRI,  $n = 17$ ) was performed. The vast majority of patients did not have medication anymore prior to SRS-T, usually for inefficacy reasons. However, the clinical evaluation was done under the pharmacological therapy (if one had such in a minority of situations), while the scanning in the drug-naïve state. The same protocol was repeated 1 year after SRS-T ( $n = 17$ ). The mean age was 70.1 years (range 49–82). The mean duration of symptoms was 38 years (range 6–70) (Table 2). The mean time to tremor improvement in the present series was 3.32 months [standard deviation (std) 2.7, range 0.5–10].

### Clinical evaluation and outcome measures

Clinical evaluation was made using validated and well-established outcome measures, every 3 months after SRS-T. Tremor severity was assessed using a questionnaire designed by Bain et al. [2] (e.g., activities of daily living (ADL)) [2], tremor score on right treated hand (TSTH, e.g., right), from Fahn-Tolosa-Marin tremor rating scale [15], and head tremor score (Table 2 for demographic data).

### Stereotactic radiosurgical thalamotomy procedure

All SRS-T procedures were performed by the same neurosurgeon (JR), using the Leksell GammaPlan software. Non-stereotactic images, including diffusion tensor diffusion data, acquired before the treatment, were co-registered with the stereotactic ones. After application of Leksell® coordinate G

**Table 1** Patient inclusion and exclusion criteria

Inclusion criteria	
•	Age between 18 and 80
•	Able to give formal approval and attend all follow-up visits (including intermediate ones at 3, 6, and 9 months)
•	Essential tremor diagnosis confirmed by our movement disorders neurologist from clinical history and examination
•	Drug resistance after adequate trials
•	Medical contraindication for DBS or radiofrequency thalamotomy
•	The Vim thalamic area apparent on MRI
Exclusion criteria	
•	Non-right-handed patients
•	Previous contralateral SRS-T
•	Previous history of stroke or epilepsy, to exclude unrelated networks appearance
•	Standard contraindication for MRI, including non-MRI compatible devices, such as cardiac pacemakers
•	Pregnancy or lactation
•	Parkinson-plus syndrome suspected on neurological examination
•	Brain tumors
•	Significant cognitive impairment, with a score at mini-mental state evaluation less or equal to 24
•	Unable to provide consent for any reason
•	Prior stereotactic and/or radiosurgery procedures in the basal ganglia area

Frame (Elekta AB, Stockholm, Sweden), all patients underwent stereotactic CT and MRI. Anterior and posterior commissure (AC and PC) were defined on the magnetic resonance ventriculography (T2 Ciss/Fiesta sequence). Indirect targeting was performed using standard methodology by Guiot's diagram, placed 2.5 mm above the AC-PC line, and 11 mm lateral to the wall of the third ventricle. A single 4-mm isocenter was used and a maximal prescription dose of 130 Gy, as well as beam blocking to optimize the gradient of dose towards the internal capsule [27, 40–42, 44].

## MRI data acquisition

Imaging was done on a head-only 3-T MRI scanner, SIEMENS SKYRA (Munich, Germany, 32-channel receive-only phased-array head coil): native (before SRS-T) and gadolinium contrast-enhanced T1-weighted (T1w, after SRS-T) and resting-state fMRI images. The following parameters were employed: T1w-TR/TE = 2300/2.98 ms, isotropic voxel of 1 mm<sup>3</sup>, 160 slices; T2\*-weighted fast echo planar imaging (BOLD contrast, before the Gadolinium injection)- TR/TE = 3.3s/30 ms/90°, voxel size 4 × 4 × 4 mm<sup>3</sup>, 300 volumes acquired per subject), 46 interleaved axial slices. The rs-fMRI experiments, acquired with no explicit task, consisted of a 10-min run, in which participants were asked to relax with their eyes closed, without falling asleep or engaging in cognitive or motor tasks. In addition, a field map was acquired to correct for the effect of field inhomogeneity.

## Resting-state fMRI data preprocessing and motion scrubbing

Processing of fMRI data was performed using different standard software suites: Statistical parametric Mapping (SPM12, <http://www.fil.ion.ucl.ac.uk/spm/>, Welcome Trust Center for Neuroimaging, London, UK). Functional scans were realigned to the first scan of the series. Since motion is an important potential confounding factor in these clinical populations, we computed Power's framewise displacement index for each time point [34]. When it exceeded 0.5 mm, the corresponding frame was "scrubbed" along with one preceding and two following ones (for a total of 5 for one time point exceeding the upper limit allowed). Only the remaining frames were further considered. At baseline, the mean number of frames taken out was 35 (median 15, range 0–135) and at 1 year was also 35 (median 15, range 0–150). Then, the images were spatially normalized into the standard anatomical space as defined by the Montreal Neurological Institute (SPM-MNI, Canada) and spatially

**Table 2** Demographic data

Variable	Mean	Standard deviation	Minimum	Maximum
Age (years)	70.1	9.8	49	82
Duration of symptoms (years)	38	19.5	6	70
ADL baseline	29.1	12	13	49
ADL (% improvement)	82.9	27.3	0	100
Right total tremor amplitude <sup>a</sup> (TSTH)	18.6	5.5	8	30
TSTH <sup>a</sup> (% improvement)	67.3	28.2	13.3	100
Head tremor score baseline (normalized)	−0.3	0.8	−1.2	0.8
Head tremor score (% improvement, normalized)	1.3	0.04	1.2	1.4
Quest baseline	46	15.1	29	80
Quest (% improvement)	24	16.1	2	47
Time to improvement after SRT (months)	3.3	2.7	0.5	10

smoothed using a Gaussian filter with a full width at high maximum (FWHM) of 6 mm. The voxel size generated from the above acquisition parameters was oversampled to  $2 \times 2 \times 2 \text{ mm}^3$ .

No sedation was used, so as not to influence resting-state brain activity in any way.

### Resting-state fMRI network extraction

Resting-state data was analyzed in Lausanne, Switzerland, by two persons not involved in patient selection, radiosurgery procedure, or follow-up course (CT and DVD).

Group-level independent component analysis (ICA) was applied to decompose rs-fMRI data into components of temporally coherent spontaneous activity using GIFT ICA Toolbox (USA, <http://icatb.sourceforge.net>) [11]. Data-driven analytic approach we employed considered the concatenated data of the 34 scans (17 subjects  $\times$  2, baseline and 1 year). Total number of components (c) was set to 20 (Table 3), which is a setting commonly used in literature for identifying large-scale distributed networks (Fig. 1). After visual inspection of maps at group level, 2 (components 1 and 3) out of 20 components were excluded. The other 18 were kept for subsequent analysis, as they showed neurologically relevant spatial pattern type (Fig. 1, Table 3).

### Resting-state fMRI statistical analysis

For rs-fMRI data, analysis of variance (ANOVA) was implemented in SPM12 (<http://www.fil.ion.ucl.ac.uk/spm/software/>

**Table 3** Identification of 18 large-scale distributed networks (common setting)

02	Right dorsal attention, in mirror with 16 (left dorsal attention)
04	Temporal pole, insula, and retrosplenial cortex
05	Cerebellar
06	Bilateral occipital and parietal
07	Brainstem
08	Brainstem and cerebellar
09	Saliency network, with frontal anterior part of the default mode network
10	Brainstem, cerebellar, and thalamic
11	Cerebellar and thalamic
12	Frontal eye fields and posterior parietal with parts of left dorsal attention
13	Bilateral motor cortex, frontal eye fields and left cerebellum lobule VI
14	Cerebellar and thalamic
15	Occipital and posterior cingulate
16	Left dorsal attention (in mirror with two, right dorsal attention)
17	Bilateral auditory and motor cortex
18	Bilateral cerebellar
19	Posterior default mode network with the posterior cingulate
20	Bilateral cerebellar and occipital

[spm12](http://spm12), London, UK) as a flexible factorial model, on each component, by using individual subject-level maps, to take into account time point (baseline versus 1 year after SRS-T), response (groups 1 and 2), and interactions between. Bonferroni correction was used to deal with number of models (20). We then report corrected *p* values using conventional cluster-level family wise error (FWE) correction.

For correlation between IC values and previously detailed tremor scores, STATA version 11 (STATA Corp LLC, College Stations, TX, USA) was used.

## Results

### Group definition for further statistical analysis

Currently available medications improve tremor in approximately 50% of patients, and propranolol, most commonly used, reduces tremor amplitude by approximately 50% [33]. To consider a therapeutical effect of SRS-T at least as effective as medication, we conventionally divided patients in two groups: 1,  $\leq 50\%$  improvement in TSTH ( $n = 6$ , 35.3%) and 2,  $> 50\%$  improvement ( $n = 11$ , 64.7%). There was no difference in age ( $p = 0.86$ ) or duration of symptoms ( $p = 0.41$ ) between groups. There was a tendency towards higher thalamotomy volumes in group 2 ( $p = 0.06$ , mean in group 1 = 0.044 ml (std 0.04, range 0.002–0.127 ml); mean in group 2 = 0.17 ml (std 0.187, range 0.027–0.600 ml).

### Clinical result

Overall ADL improvement was 82.9% (std dev 27.3, range 0–100%), and TSTH improvement was 67.3% (std dev 28.2, range 13.3–100%).

### Radiological outcome: lesion volume after thalamotomy

The thalamotomy volume has been drawn on the T1 (gadolinium-injected) MR, 1 year after SRS-T, which is considered the definitive radiological answer in our experience [43]. To ensure the accuracy of this volume calculation, each patient MR at 1-year follow-up was imported in the Leksell GammaPlan software (Elekta instruments, AB, Sweden) and co-registered with the therapeutic images. We projected on the MR-signature the 90-Gy isodose line, which corresponds to the final radiological response, in our previously published experience [35, 43]. Manually, using the segmentation tools, the draw was made for the individual cases. The “volume” module inside the station was used to extract the values.

Mean lesion volume after SRS-T was 0.125 ml (std 0.162, range 0.002–0.600 ml). There was no correlation between

ADL drop and lesion volume ( $p = 0.17$ ), but the former related with TSTH improvement ( $p = 0.04$ ).

### Cognitive assessment

Mean pretherapeutic Matthis Dementia Rating Scale [38] was 135.9, and post-therapeutic was 135.5 ( $p > 0.05$ ).

### Interaction between time point (baseline versus 1 year) and clinical response

**Relevant regions: IC strength between default mode network and bilateral insula (c9) with left claustrum and putamen (1) and bilateral motor cortex (c13) with right visual association cortex (2)**

We report statistically significant IC within two networks. The first is salience, involving bilateral superior frontal gyri and insular areas (c9) with left claustrum and putamen (Fig. 2(2.1.–2.4); Fig. 3 for brief anatomical relevance). The second

is bilateral motor network, frontal eye fields and left cerebellum lobule VI (c13) with right visual association cortex, right Brodmann area (BA) 19 (Table 4; Fig. 4(4.1–4.6); Fig. 5 for brief neuroanatomical relevance).

For the left claustrum and putamen, corresponding boxplots and their median IC values are shown in Fig. 2 (for IC values, refer to Table 5). At baseline, IC values were positive in group 1 and remained further so, while being close to zero in group 2 (Fig. 2(2.1)). Functional interconnectivity differences (between 1 year and baseline) were actually related to TSTH improvement, allowing a separation of group 1 from group 2 (Fig. 2(2.2)). An increase in IC at 1 year was associated with a better outcome (Fig. 2(2.2)). Furthermore, baseline IC correlated with the TSTH improvement percentage, from a range of 1.91 (13.3% improvement) to  $-0.46$  (100% improvement) (Spearman's rank correlation coefficient = 0.01, Fig. 2(2.3)). Shorter disease duration was associated with better TSTH improvement and an IC value increases at 1 year, towards 1 (Fig. 2(2.4)) (Spearman's rank correlation coefficient = 0.02).

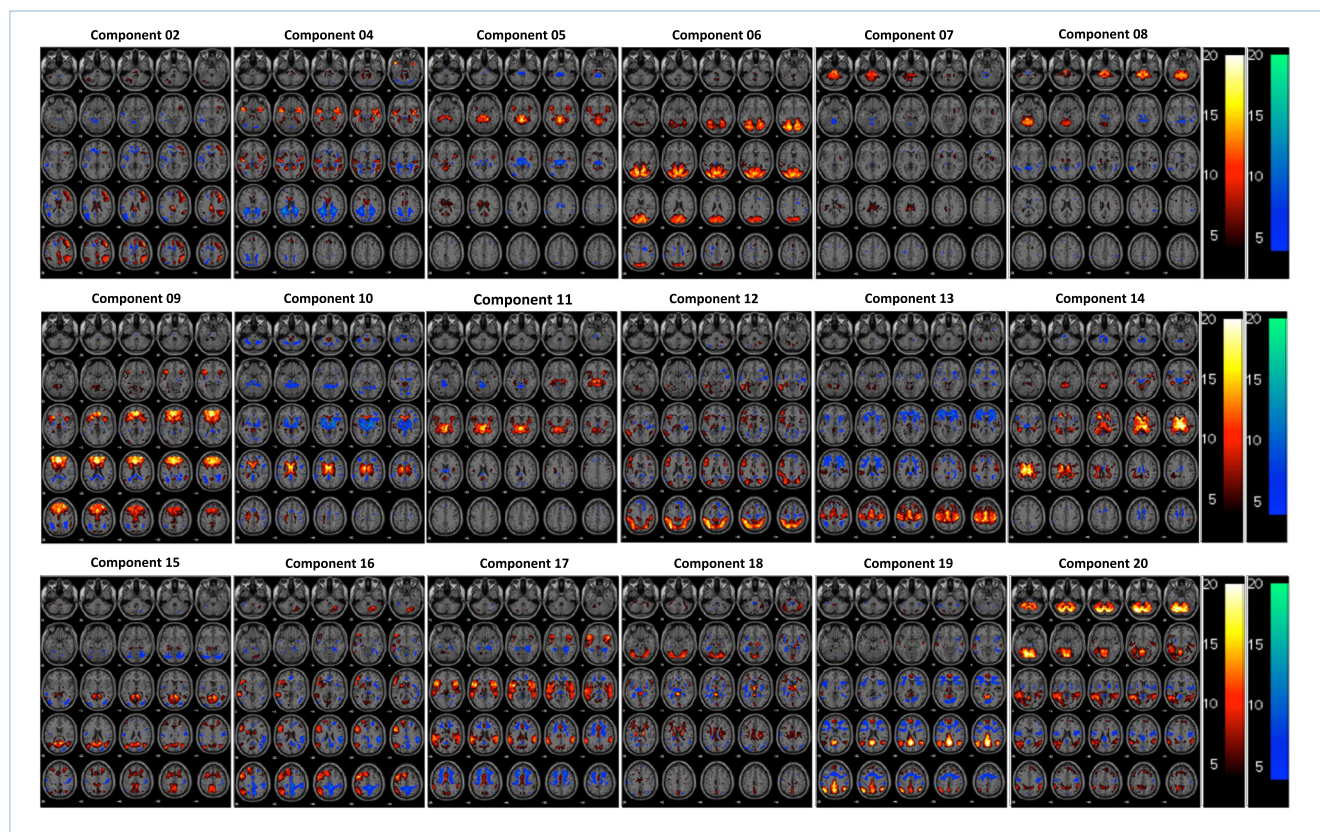


**Fig. 1** A total number of 20 components (c) with their respective networks were separated using visual evaluation both of their spatial profile and time course: c2, right dorsal attention, in mirror with c16, left dorsal attention; c4, temporal pole, insula and retrosplenial cortex; c5, cerebellar; c6, bilateral occipital and parietal; c7, brainstem; c8, brainstem and cerebellar; c9, the frontal anterior part of the default mode network (DMN);

c10, cerebellar and thalamic; c11, cerebellar and thalamic; c12, frontal eye fields and posterior parietal; c13, bilateral motor cortex, frontal eye fields and left cerebellum lobule VI; c14, cerebellar and thalamic; c15, occipital and posterior cingulate; c17, bilateral auditory and motor cortex; c18, bilateral cerebellar; c19, posterior DMN with the posterior cingulate; c20, bilateral cerebellar and occipital

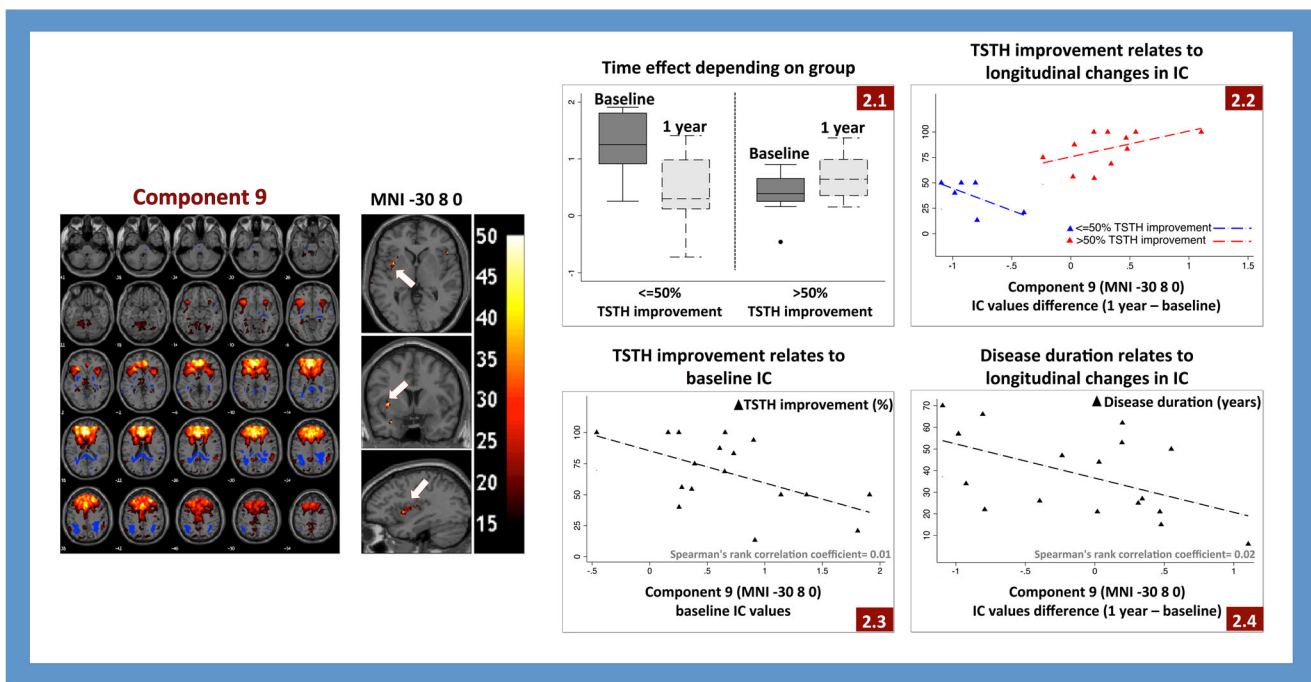


**Fig. 2** Interaction group (TSTH improvement  $\leq 50\%$  or  $> 50\%$ ) with time (baseline versus 1 year after SRS-T); component 9, with insula and default mode network IC with left claustrum and putamen. 2.1: boxplots with the median values for IC values corresponding to the left claustrum and putamen; 2.2: differences in IC between 1 year and

baseline clearly separate the two groups, 1 and 2, and are statistically significant; 2.3: baseline IC values additionally correlate with baseline TSTH (Spearman = 0.01); 2.4: differences in IC, 1 year after SRS-T, correlate with disease duration (Spearman = 0.02)

For right visual association area, corresponding boxplots and their median values are shown in Fig. 4. The IC values can be seen in detail in Table 5. At baseline, they were negative in group 1 and inversely positive at 1 year, while in group 2 had already positive pretherapeutic values (which decreased to a median of zero one year later)(Fig. 4(4.1)). A decrease in IC at 1 year was related to TSTH improvement, allowing a separation of group 1 from group 2 (Fig. 4(4.2)). The baseline IC values predicted percentage of TSTH improvement, with

positive values associated with a better outcome (range from  $-1.068$  (13.3% improvement) to  $1.065$  (100% improvement)) (Spearman’s rank correlation coefficient = 0.01, Fig. 4(4.3)). Furthermore, baseline head tremor score (Fig. 4(4.4)) correlated with baseline IC values (negative IC associated for both with higher tremor scores for both, Spearman’s rank correlation coefficient = 0.02). Interestingly, higher lesion volumes were associated both with higher difference in IC values between 1 year and baseline (Fig. 4(4.5), Spearman’s rank

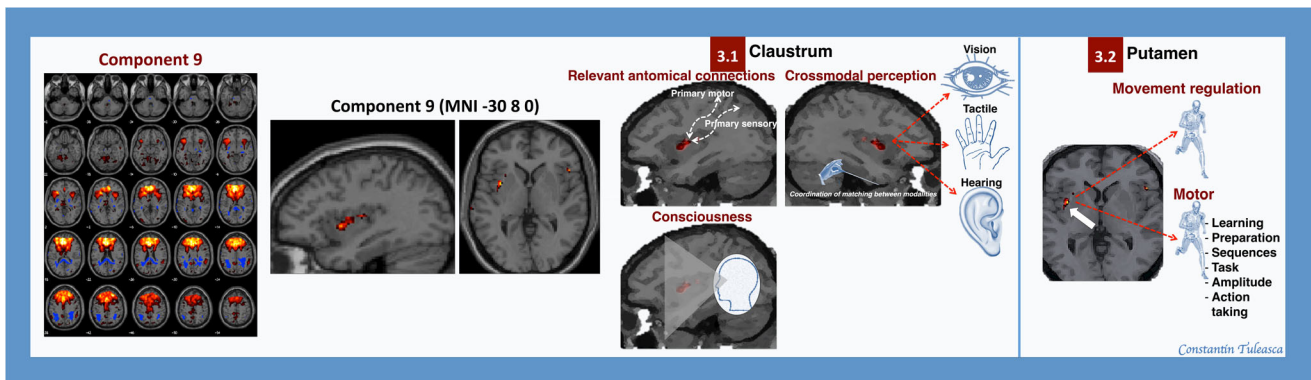


**Fig. 3** Artistic representation of the findings from the interaction group with time, as presented in Fig. 2; the respective roles of the relevant clusters are briefly synthesized: 3.1, the claustrum; 3.2, the putamen

**Table 4** Interconnectivity results with the statistically significant anatomical regions

	Anatomical region	MNI	<i>p</i> uncorrected	<i>p</i> FWE corrected	<i>K</i> <sub>c</sub>	Peak level
The interaction between the group and the time point						
Component 9	Left claustrum and putamen	−30 8 0 −34 −4 4 −24 14 0	0.000	0.001	86	4.43 4.09 4.09
Component 13	Right BA 19 (visual associative)	32 −80 10	0.000	0.001	87	5.66
The main effect of time point (baseline versus 1 year after SRT)						
Component 2	Ventrolateral prefrontal cortex (including BA 45 44)	−26 22 22 −20 38 10 −16 30 16	0.000	0.000	140	4.49 4.46 4.17
Component 9	Fusiform gyrus (includes parts of V5)	50 −62 −8 46 −78 −2	0.000	0.000	115	4.69 3.60

correlation coefficient = 0.001) and also with higher baseline IC values (Fig. 4(4.6), Spearman's rank correlation coefficient = 0.01).

### Main effect of time point (baseline versus 1 year after SRS-T)

**Relevant anatomical regions: IC strength between right dorsal attention network (c2) with left anterior ventro-lateral prefrontal cortex (1); reminiscent salience network (c9) with right fusiform gyrus (including V5) (2)**

We report statistically significant IC within two networks. The first is right dorsal attention network (c2) with the left anterior ventro-lateral prefrontal cortex (VLPFC, Fig. 6(6.1–6.3); Fig. 7 for brief anatomical relevance). The second is a reminiscent salience network (c9) IC with fusiform gyrus (Fig.

8(8.1, 8.2)) with a cluster including parts of right visual area V5 (Fig. 9 for brief anatomical relevance, Tables 3 and 4).

For the VLPFC (Fig. 6(6.1, 6.2) for their respective values), no or slight change in IC at 1 year after SRS-T correlated with better TSTH improvement (Spearman's rank correlation coefficient = 0.01, Fig. 6(6.3)).

For the right fusiform gyrus and visual area V5 (Fig. 8(8.1, 8.2)), the mean baseline IC values in group 1 were 0.33 (−1 to 1.10) and at 1 year passed to −0.30 (−0.69 to 0.28); for group 2, the mean was 0.02 (−0.86 to 0.93) and at 1 year passed to 0.27 (−1.07 to 2.46) (Fig. 8(8.1, 8.2)). In this sense, overall interconnectivity values decreased from slightly positive to the opposite slightly negative values; furthermore, patients who alleviated less presented slightly positive pretherapeutic interconnectivity (which decreased to a median symmetric slightly negative value (close to zero) 1 year later), while those who alleviated more had pretherapeutic negative median

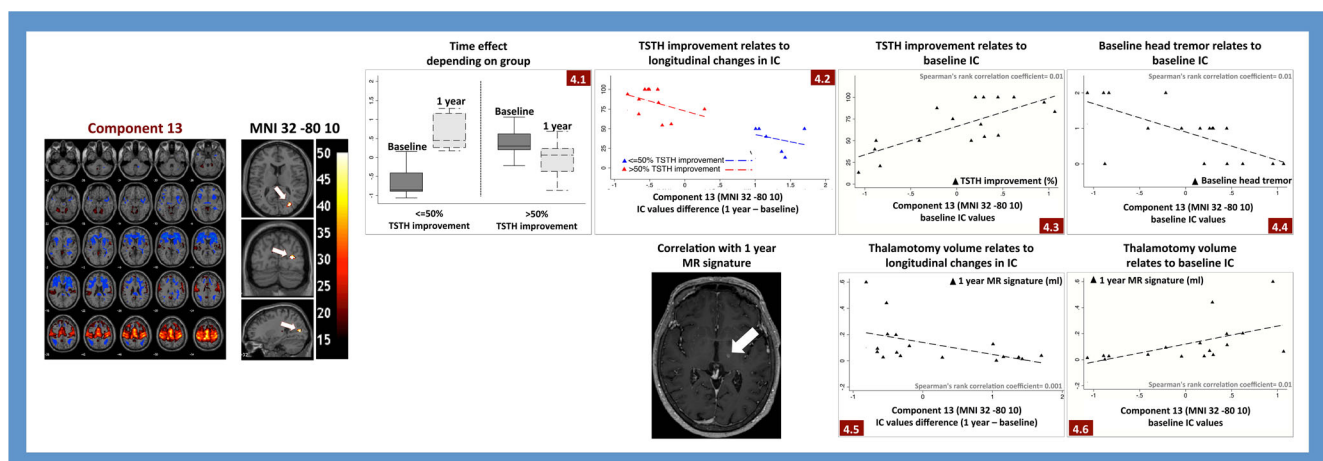


**Fig. 4** Component 13, with bilateral sensorimotor cortex frontaleye fields and left cerebellum lobule VI, IC with right visual association area. 4.1: boxplots with the median values for corresponding IC values for right visual association area; 4.2: differences in IC between 1 year and baseline clearly separate the two groups, 1 and 2, and are statistically

significant; 4.3: baseline IC values correlate with TSTH improvement (Spearman = 0.01); 4.4: baseline IC values correlate with baseline head tremor score (Spearman = 0.01); 4.5: differences in IC at 1 year after SRS-T correlate with lesion volume (Spearman = 0.001); 4.6: baseline IC also correlate with lesion volume (Spearman = 0.01)

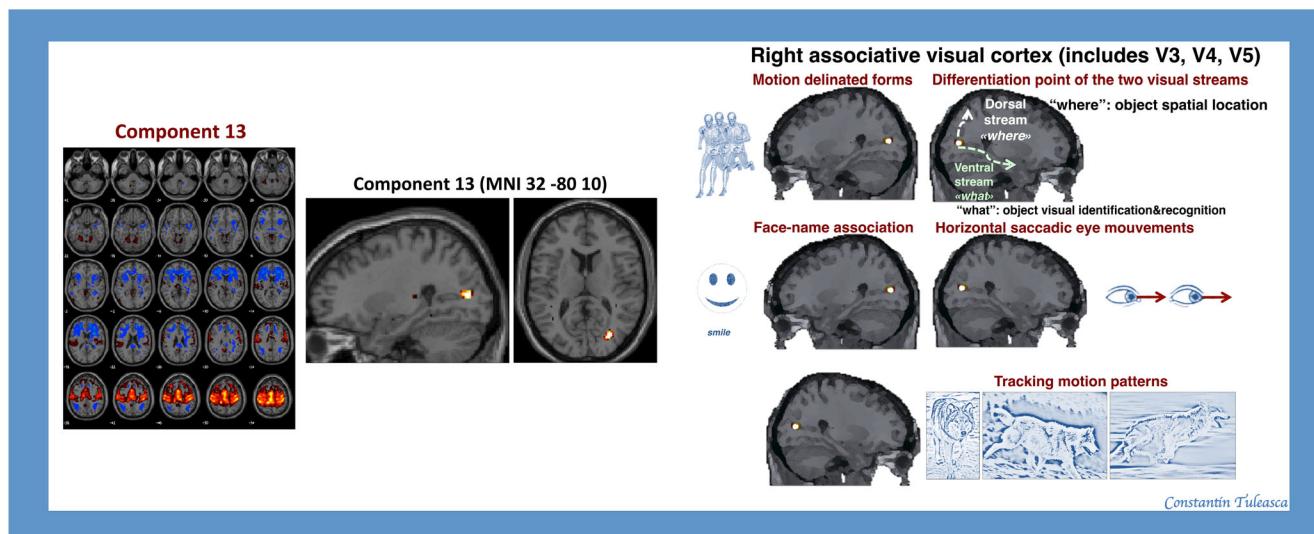


**Fig. 5** Artistic representation of the findings from interaction group with time, as presented in Fig. 4; the respective roles of the relevant cluster are briefly synthesized: right visual association cortex

values (close to zero, which slightly increased to a median of zero 1 year later). These results are at the opposite with those presented in Fig. 4(4.1), reflecting the interconnectivity between the bilateral motor network, frontal eye fields, and left cerebellum lobule VI with right BA 19.

**Main effect of group (group 1 versus 2, independent of time point)**

Multiple differences were found between group 1 and group 2, independent of time point, involving the following relevant anatomical regions: the cerebellum (comprising dentate nucleus), basal ganglia including thalamus (both right and left) and putamen, frontal lobe (encompassing frontal eye fields, dorso-lateral prefrontal cortex), parietal lobe (angular and supramarginal gyrus), temporal lobe (middle temporal area), occipital lobe (visual association areas, retrosplenial cortex), cingulate (both anterior dorsal and posterior). They are displayed

in supplementary Figs. 1, 2, 3 (Fig. 10 for neuro-anatomical relevance) and Table 6. The corresponding boxplots present median values as well as the range for each group, at baseline and 1 year after SRS-T.

**Influence of confounders**

For relevant IC values, there was no influence of age ( $p > 0.05$ ). The influence of disease duration was statistically significant only for c9 (see below). The thalamotomy volume correlated only with IC strength between bilateral motor areas (c13) with right visual association area (see the respective section of the manuscript).

**Discussion**

To the best of our knowledge, this is the first study that uses rs-fMRI as a non-invasive neuro-imaging tool for evaluating

**Table 5** Interconnectivity values allows separating two groups (1 and 2)

Interaction between the group and time point		Mean	Standard deviation	Min	Max
Component 9 FC at baseline	Group 1	1.23	0.61	0.26	1.91
left claustrum and putamen	Group 2	0.41	0.37	-0.46	0.90
Component 9 difference (1-year baseline)	Group 1	-0.83	0.24	-1.10	-0.40
left claustrum and putamen	Group 2	0.31	0.35	-0.24	1.10
Component 13 FC at baseline	Group 1	-0.65	0.45	-1.07	0.16
right visual associative cortex	Group 2	0.39	0.38	-0.22	1.06
Component 13 FC difference (1-year baseline)	Group 1	1.29	0.26	1.01	1.70
right visual associative cortex	Group 2	-0.43	0.29	-0.81	0.28



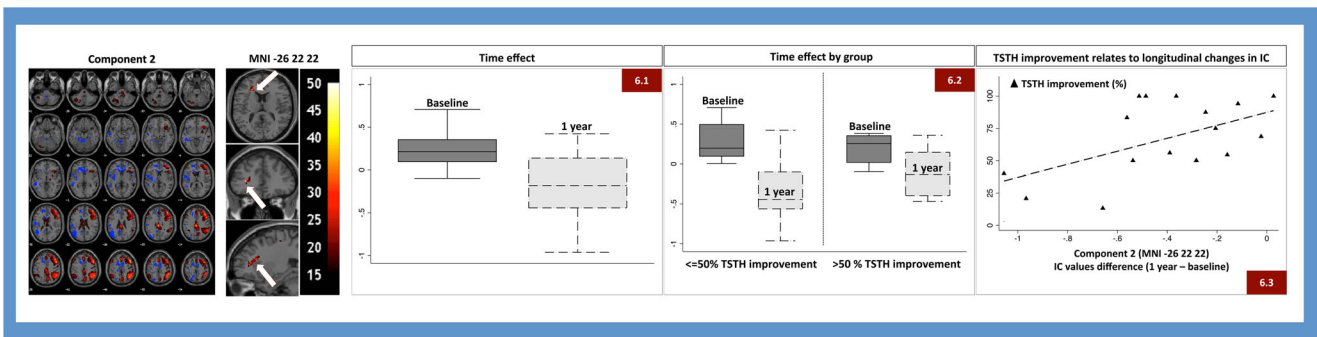


**Fig. 6** Illustration of time-effect (baseline versus 1 year after SRS-T): Component 2, with right dorsal attention IC with left anterior VLPFC. 6.1: boxplots with the median values for corresponding IC values for left

anterior VLPFC, as overall changes between baseline and 1 year after SRS-T and further 6.2, separated by groups; 6.3: TSTH improvement relates to longitudinal changes in IC

clinical response after SRS-T. We considered both baseline and 1 year after SRS-T follow-up functional imaging, to be able to detect network changes related to therapeutic answer after SRS-T. We focused on improvement in TSTH, as SRS-T was performed only unilaterally in this cohort (left SRS-T for right hand).

We report TSTH improvement correlated with IC strength between salience network with the left claustrum and putamen, as well as between the bilateral motor cortex, frontal eye fields and left cerebellum lobule VI with right visual association area (former also with lesion volume). Longitudinal changes showed additional associations in IC strength between right dorsal attention network with ventro-lateral prefrontal cortex and salience network with fusiform gyrus. Relevant networks are visual, motor, and attention. Interconnectivity between visual and motor areas is a novel finding, revealing implication in movement sensory guidance, as well as the presence of a widespread cerebello-visuo-motor

resting-state functional network, which is related to clinical effect after Vim SRS-T for ET.

We briefly analyzed the neuroanatomical perspective of these relevant brain areas. The input and output of the claustrum are related to almost all regions of the cortex (including cingulate, visual areas in occipital lobe, entorhinal cortex, and temporal areas) [14]. Furthermore, we identified that the anterior dorsal part, found here, connects with motor and somato-sensory cortex. Main functions include cross-modal perception [12], coordination of matching between visual and tactile modalities [3], and has even been invoked as important to consciousness [14]. The putamen, by its connections to the substantia nigra and globus pallidus, plays a major role in movement regulation, motor learning, preparation, sequences, tasks and amplitude, limb movement control, and as part of the motor system that is mobilized to take action, or influences various types of learning [1]. Right visual association cortex (including V3, V4, V5) was interconnected with c13, bilateral

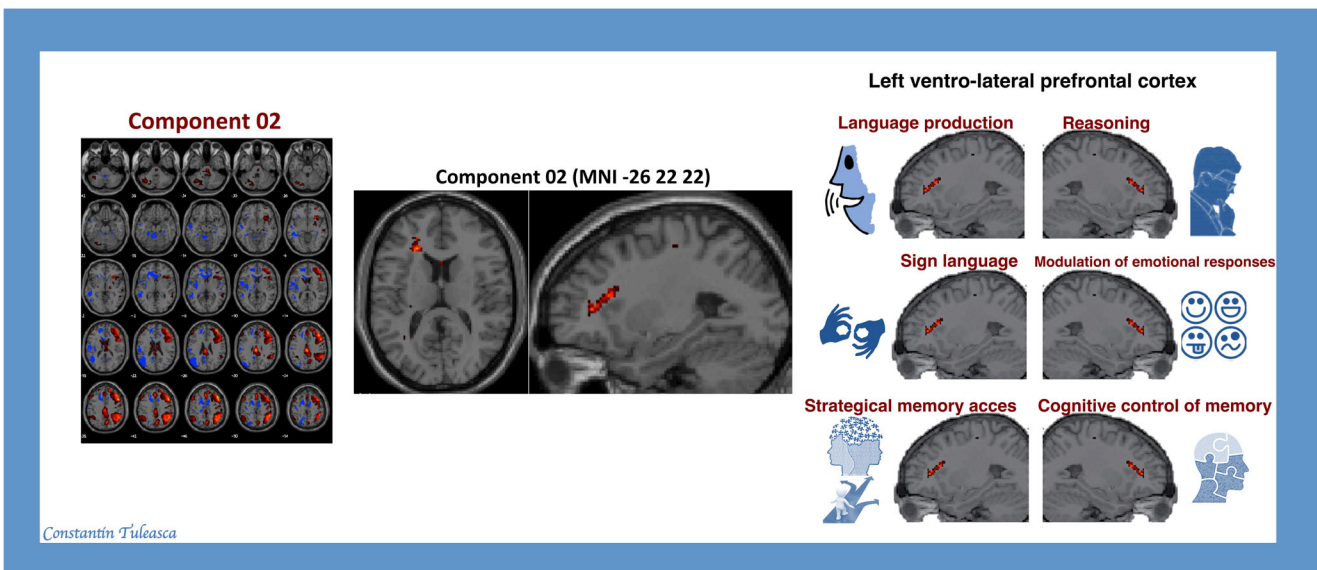


**Fig. 7** Artistic representation of the findings from the main effect of time point, as presented in Fig. 6; the respective roles of the relevant clusters are briefly synthesized: left ventro-lateral prefrontal cortex

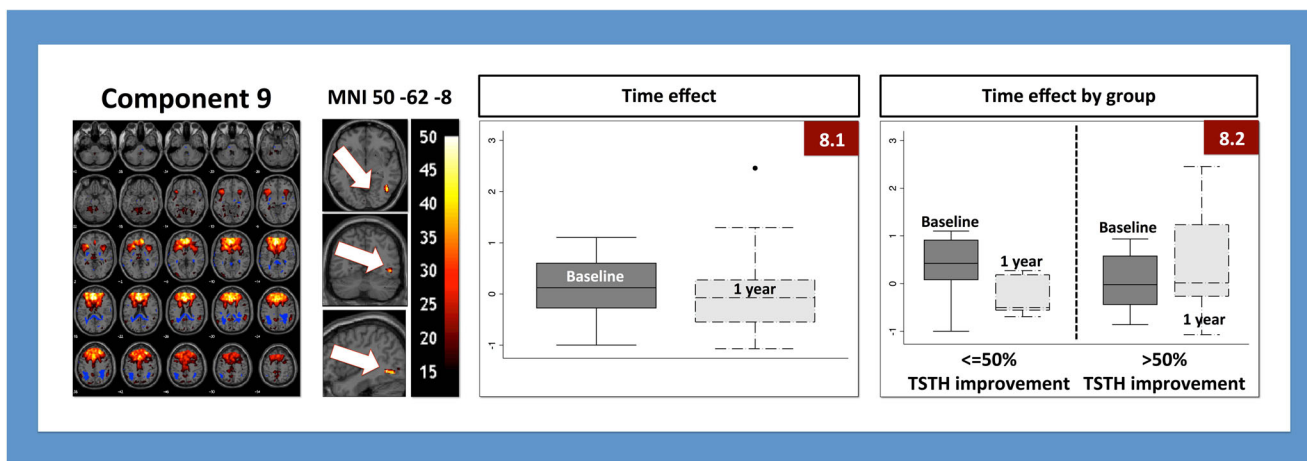


**Fig. 8** Component 9, with bilateral insula and default mode network IC with the corresponding right visual association area (including V5); 8.1: boxplots with the median values for corresponding IC values for left anterior VLPFC, as overall changes between baseline and 1 year after

SRS-T and further 8.2, separated by groups; for 8.2., opposite results are observed as compared with the figure 4.1, reflecting the interconnectivity between the bilateral motor network with right BA 19

motor network, frontal eye fields and left cerebellum lobule VI component. It has been previously hypothesized that visual areas must be linked to motor areas for sensory guidance of movement of hand and fingers [21], and further so in motor control. Several hypotheses warrant for further discussion. One possibility would be that corpus callosum actually mediates tasks in which the visual cortex on one part of the body is linked to the contralateral motor cortex, in line with our findings. Another hypothesis would be visual input to the caudate nucleus and claustrum [37], explaining appearance of the former in another component (see previous). Furthermore, a third possibility could be that the cerebellum might play the essential role of calibrating the relationship between visual and somatosensory/motor information. Other functions of the visual association cortex are related to feature extraction,

attentional and multimodal integrating functions. Furthermore, electrophysiology data suggest sensitivity to motion-delineated forms [39] and its role as a differentiation point between the “what” and “where” visual pathways. Additional involvement of the visual association cortex is in horizontal saccadic eye movements, visuospatial information processing, orientation-selective attention, and tracking visual motion patterns [45].

The left VLPFC is considered the end-point of ventral pathway, which brings information about stimuli characteristics. In the present study, it is interconnected with the right dorsal attention network. Recent studies have suggested a role in hand movements [36]. The fusiform gyrus, interconnected here with salience network, is mainly involved in high-level vision as part of the ventral visual stream (“what” pathway)

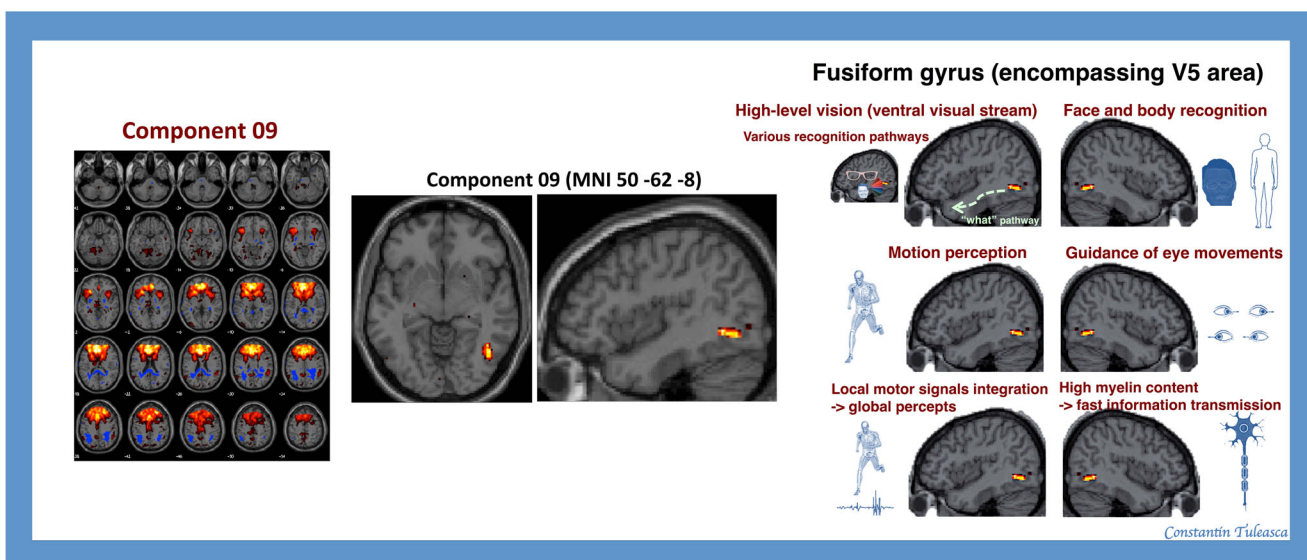


**Fig. 9** Artistic representation of the findings from the main effect of time point, as presented in Fig. 8; the respective roles of the relevant cluster are briefly synthesized: fusiform gyrus

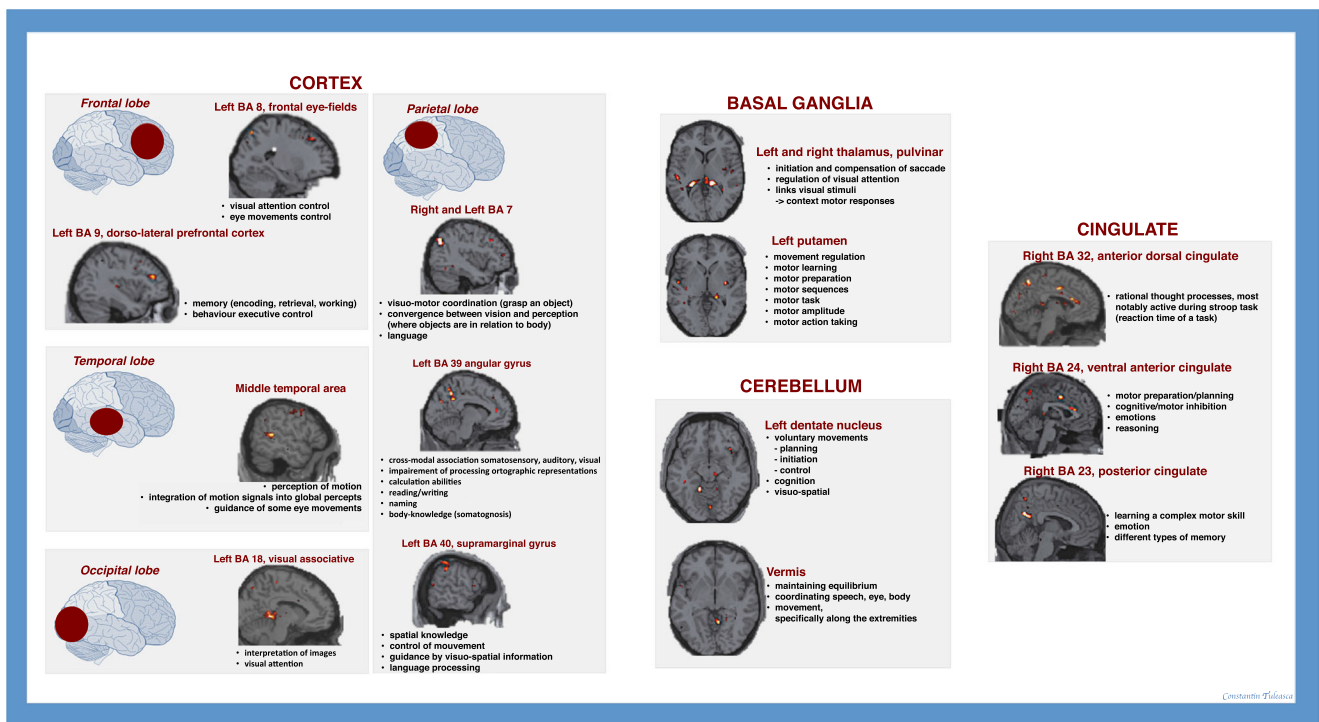


**Fig. 10** Artistic representation of the main findings from main effect of group, as presented in supplementary Figs. 1, 2 and 3; the respective roles of the relevant anatomical areas are briefly synthesized

and various neural pathways related to recognition. It encompasses the middle temporal area (V5) and plays a major role in motion perception, integration of local motor signals into global percepts, and guidance of some eye movements. Major projections include eye movement-related areas (e.g., frontal eye fields). It is worth noting that both V5 and V6 have high myelin content, a characteristic that is usually present in brain structures involved in fast information transmission.

Essential tremor is currently considered a spectrum of clinical features, including both motor and non-motor elements [31]. These features are nicely represented by found group differences, involving multiple anatomical regions (Fig. 6).

Only one previous study, not related to radiosurgery [24], evaluated the effect of Vim HIFU in 10 patients with drug-resistant ET, on brain networks. A major difference is that Vim HIFU produces an apparent lesion and clinical effect immediately, unlike SRS-T (with MR signature and clinical effect which can develop up to 1 year after the procedure). This delayed effect could account for brain networks reorganization and plasticity. The authors of the HIFU study used graph analysis on rs-fMRI data and found whole brain effects/changes at a later time point of 3 months after the intervention, on the right lateral inferior occipital cortex. Part of this cluster also appeared in the present study. Resting-state observational studies in ET, which are non-interventional, are not the primary focus of the present report [5, 10, 16–18, 28].

We used a data-driven method (i.e., ICA) that allows identifying resting-state networks without any a priori

hypothesis. We did this so as to not evaluate a specific tremor network, nor probe the cerebello-thalamo-cortical pathway, which was beyond our purpose. While one would expect that Vim “suppression” by SRS-T has an impact only on the known motor and/or tremor network(s), we presently report changes within remote areas, including purely motor, visuomotor areas, and areas related to cognition and attention. These network changes 1 year after SRS-T are related to tremor improvement. In this sense, they might play a major, underestimated, physiopathological role, either because of a particular baseline phenotype [31], or by adaptive changes to intervention itself.

We reported an interesting connection between visual association areas and left cerebellum lobule VI- frontal eye fields and motor cortex in our ET patients, in the clinical context of impairment of sensory guidance of movements, including of hand and fingers. In fact, additional visual attention deficits or dysfunction in hand-eye coordination and ocular movements is considered as non-motor features in ET [6]. It is known that visual attention is of high importance for visual perception and for all the things we put perception to, including learning, memory, and our interactions with the visual world [7]. It is worth noting that top-down signals come from multiple frontal and parietal regions, but their “competition” is ultimately resolved within the visual cortex [25].

**Table 6** The main effect of group (short overview)

The main effect of the group (TSTH $\leq$ 50% versus RTTA $>$ 50%)						
	Anatomical region (BA = Brodmann)	MNI	<i>p</i> uncorrected	<i>p</i> FWE corrected	<i>Kc</i>	Peak level
Component 5	Left dentate nucleus	-10 -52 -10	0.000	0.004	65	82.27
	Vermis	6 -48 2	0.000	0.000	105	68.60
	Right thalamus (pulvinar)	12 -28 6	0.000	0.000	140	57.18
Component 6	Right BA 7, parietal	8 -68 32	0.000	0.000	104	58.57
Component 11	Right thalamus	18 -36 4	0.000	0.000	268	220.45
	Left thalamus	-18 -36 4	0.000	0.000	200	99.21
	Right putamen	38 -8 -2	0.000	0.000	111	57.52
Component 12	Left BA 39, angular gyrus	-44 -58 46	0.000	0.000	271	123.14
	Left visual associative	-4 -42 0	0.000	0.000	198	63.08
	Left BA 7, parietal	-6 -72 50	0.000	0.002	81	56.83
	Left BA 37, fusiform gyrus	-24 -38 -14	0.000	0.003	74	56.34
	Left BA 7, parietal	-20 -70 32	0.000	0.000	235	56.25
	Left BA 19, occipital	-52 -66 0	0.000	0.000	231	41.30
	Right BA 7, parietal	8 -70 44	0.000	0.000	114	34.36
Component 13	Right BA 40, supramarginal gyrus	52 -36 38	0.000	0.000	103	100.08
	Left BA 9, dorso-lateral pre-frontal	-30 32 22	0.000	0.000	99	77.11
	Left BA 8, frontal eye fields	-26 24 50	0.000	0.004	73	42.96
	Left BA 40, supramarginal gyrus	-58 -34 30	0.000	0.006	68	40.82
Component 15	Left BA 23, retrosplenial cortex	-22 -58 8	0.000	0.000	147	117.81
	Left BA 39, angular gyrus	-56 -54 26	0.000	0.000	127	49.69
Component 16	Right BA 23, posterior cingulate	10 -54 24	0.000	0.000	132	102.21
	Left BA 21, middle temporal area	-46 -44 10	0.000	0.000	113	74.10
	Left BA 40, supramarginal gyrus	-56 -38 36	0.000	0.000	109	36.54
Component 18	Left BA 39, angular gyrus	-46 -42 28	0.000	0.000	143	154.60
	Left BA 7, parietal	-8 -66 60	0.000	0.000	197	106.90
	Left cerebellar	-42 -60 24	0.000	0.000	259	90.01
	Right BA 32, anterior dorsal cingulate	4 -2 42	0.000	0.002	76	75.56
	Right BA 39, angular gyrus	40 -58 50	0.000	0.003	75	65.53
Component 19	Right BA 24, ventral anterior cingulate	2 28 16	0.000	0.000	100	57.37
	Left BA 7, parietal	-28 -66 50	0.000	0.000	107	95.73
	Left BA 39, angular gyrus	-38 -72 34	0.000	0.000	105	94.19
	Left BA 32, anterior dorsal cingulate	-2 40 12	0.000	0.000	101	63.38

Our study has several potential limitations. One is the small number of subjects. Another, related to study design, is the use of resting-state data, which might not be directly related to motor performance; however, we aimed at studying network changes in the absence of a task. A third one is the lack of data on longitudinal changes (at baseline and 1 year) in a healthy control group; nevertheless, recent studies have advocated the reproducibility of functional networks across multiple sessions, including 1 year apart [23]. Furthermore, neurological evaluation was not blinded. Also, at which exact time point SRS-T induces these changes in brain networks remains unknown. The anatomical location of some clusters, such as the claustrum, should be carefully interpreted, due to the relatively low resolution of the fMRI in general.

## Conclusion

In conclusion, we report that a focal Vim lesion, produced by SRS-T, is correlated with a distinct functional connectivity pattern, implying changes not only within parts of the pure widely known motor loop, but also on remote areas, including primarily motor (the claustrum, putamen; interconnected with salience network) and visual (occipital association cortex; interconnected with left cerebellum lobule VI, frontal eye fields and bilateral motor cortex) area. Using longitudinal data, at baseline and 1 year after SRS-T, we suggest that rs-fMRI relates to clinical response. The main areas involved include motor and visual networks, (but also cognitive and attention responsible regions, mainly involved in attention (e.g., salience, dorsal attention)), suggesting the connection between the former in sensory guidance of movements of hands and fingers.

**Acknowledgments** We acknowledge the contribution of Axelle Cretol, from Marseille University Hospital (CHU Timone), France, who, as a research assistant, kept the database up-to-date.

**Funding** The work was supported by the Swiss National Science Foundation (SNSF-205321-157040) and by the Centre d'Imagerie BioMédicale (CIBM) of the University of Lausanne (UNIL), the Swiss Federal Institute of Technology Lausanne (EPFL), the University of Geneva (UniGe), the Centre Hospitalier Universitaire Vaudois (CHUV), the CHU Timone, Marseille, France, the Hôpitaux Universitaires de Genève (HUG), and the Leenaards and Jeantet Foundations.

## Compliance with ethical standards

**Conflict of interest** The authors declare that they have no conflict of interest.

**Ethics approval** The Ethical Committee of the Marseille University Hospital (CPPRB1) approved our study.

## References

- Alexander GE, Crutcher MD (1990) Functional architecture of basal ganglia circuits: neural substrates of parallel processing. *Trends Neurosci* 13:266–271
- Bain PG, Findley LJ, Atchison P, Behari M, Vidailhet M, Gresty M, Rothwell JC, Thompson PD, Marsden CD (1993) Assessing tremor severity. *J Neurol Neurosurg Psychiatry* 56:868–873
- Banati RB, Goerres GW, Tjoa C, Aggleton JP, Grasby P (2000) The functional anatomy of visual-tactile integration in man: a study using positron emission tomography. *Neuropsychologia* 38:115–124
- Benabid AL, Pollak P, Gao D, Hoffmann D, Limousin P, Gay E, Payen I, Benazzouz A (1996) Chronic electrical stimulation of the ventralis intermedialis nucleus of the thalamus as a treatment of movement disorders. *J Neurosurg* 84:203–214
- Benito-Leon J, Louis ED, Romero JP, Hernandez-Tamames JA, Manzanedo E, Alvarez-Linera J, Bermejo-Pareja F, Posada I, Rocon E (2015) Altered functional connectivity in essential tremor: a resting-state fMRI study. *Medicine* 94:e1936
- Bermejo-Pareja F, Puertas-Martin V (2012) Cognitive features of essential tremor: a review of the clinical aspects and possible mechanistic underpinnings. *Tremor Other Hyperkinet Mov* 2:
- Bisley JW (2011) The neural basis of visual attention. *J Physiol* 589:49–57
- Biswal B, Yetkin FZ, Haughton VM, Hyde JS (1995) Functional connectivity in the motor cortex of resting human brain using echoplanar MRI. *Magn Reson Med* 34:537–541
- Blomstedt P, Hariz GM, Hariz MI, Koskinen LO (2007) Thalamic deep brain stimulation in the treatment of essential tremor: a long-term follow-up. *Br J Neurosurg* 21:504–509
- Buijink AW, van der Stouwe AM, Broersma M, Sharifi S, Groot PF, Speelman JD, Maurits NM, van Rootselaar AF (2015) Motor network disruption in essential tremor: a functional and effective connectivity study. *Brain J Neurol* 138:2934–2947
- Calhoun VD, Adali T, Pearlson GD, Pekar JJ (2001) A method for making group inferences from functional MRI data using independent component analysis. *Hum Brain Mapp* 14:140–151
- Calvert GA (2001) Crossmodal processing in the human brain: insights from functional neuroimaging studies. *Cereb Cortex* 11:1110–1123
- Campbell AM, Glover J, Chiang VL, Gerrard J, Yu JB (2015) Gamma knife stereotactic radiosurgical thalamotomy for intractable tremor: a systematic review of the literature. *Radiother Oncol* 114:296–301
- Crick FC, Koch C (2005) What is the function of the claustrum? *Philos Trans R Soc Lond Ser B Biol Sci* 360:1271–1279
- Fahn S, Tolosa E, Marin C (1988) Clinical rating scale for tremor. *Parkinson's disease and movement disorders*. Urban and Schwarzenberg, Baltimore, pp 225–234
- Fang W, Chen H, Wang H, Zhang H, Liu M, Puneet M, Lv F, Cheng O, Wang X, Lu X, Luo T (2015) Multiple resting-state networks are associated with tremors and cognitive features in essential tremor. *Mov Disord* 30:1926–1936
- Fang W, Chen H, Wang H, Zhang H, Puneet M, Liu M, Lv F, Luo T, Cheng O, Wang X, Lu X (2016) Essential tremor is associated with disruption of functional connectivity in the ventral intermediate nucleus—motor cortex—cerebellum circuit. *Hum Brain Mapp* 37:165–178
- Fang W, Lv F, Luo T, Cheng O, Liao W, Sheng K, Wang X, Wu F, Hu Y, Luo J, Yang QX, Zhang H (2013) Abnormal regional homogeneity in patients with essential tremor revealed by resting-state functional MRI. *PLoS One* 8:e69199

19. Fox MD, Raichle ME (2007) Spontaneous fluctuations in brain activity observed with functional magnetic resonance imaging. *Nat Rev Neurosci* 8:700–711
20. Gallea C, Popa T, Garcia-Lorenzo D, Valabregue R, Legrand AP, Marais L, Degos B, Hubsch C, Fernandez-Vidal S, Bardinet E, Roze E, Lehericy S, Vidailhet M, Meunier S (2015) Intrinsic signature of essential tremor in the cerebello-frontal network. *Brain J Neurol* 138:2920–2933
21. Glickstein M (2000) How are visual areas of the brain connected to motor areas for the sensory guidance of movement? *Trends Neurosci* 23:613–617
22. Goldman MS, Ahlskog JE, Kelly PJ (1992) The symptomatic and functional outcome of stereotactic thalamotomy for medically intractable essential tremor. *J Neurosurg* 76:924–928
23. Guo CC, Kurth F, Zhou J, Mayer EA, Eickhoff SB, Kramer JH, Seeley WW (2012) One-year test-retest reliability of intrinsic connectivity network fMRI in older adults. *NeuroImage* 61:1471–1483
24. Jang C, Park HJ, Chang WS, Pae C, Chang JW (2016) Immediate and longitudinal alterations of functional networks after thalamotomy in essential tremor. *Front Neurol* 7:184
25. Kastner S, Ungerleider LG (2000) Mechanisms of visual attention in the human cortex. *Annu Rev Neurosci* 23:315–341
26. Kondziolka D, Ong JG, Lee JY, Moore RY, Flickinger JC, Lunsford LD (2008) Gamma knife thalamotomy for essential tremor. *J Neurosurg* 108:111–117
27. Lefranc M, Carron R, Regis J (2015) Prelemniscal radiations: a new reliable landmark of the thalamic nucleus ventralis intermedialis location. *Stereotact Funct Neurosurg* 93:400–406
28. Lenka A, Bhalsing KS, Panda R, Jhunjhunwala K, Naduthota RM, Saini J, Bharath RD, Yadav R, Pal PK (2017) Role of altered cerebello-thalamo-cortical network in the neurobiology of essential tremor. *Neuroradiology* 59:157–168
29. Lipsman N, Schwartz ML, Huang Y, Lee L, Sankar T, Chapman M, Hynynen K, Lozano AM (2013) MR-guided focused ultrasound thalamotomy for essential tremor: a proof-of-concept study. *Lancet Neurol* 12:462–468
30. Louis ED (2005) Essential tremor. *Lancet Neurol* 4:100–110
31. Louis ED (2009) Essential tremors: a family of neurodegenerative disorders? *Arch Neurol* 66:1202–1208
32. Louis ED (2016) Essential tremor with head tremor: trait or state? *J Can Sci Neurol* 43:443–444
33. Lyons KE, Pahwa R (2008) Pharmacotherapy of essential tremor: an overview of existing and upcoming agents. *CNS Drugs* 22:1037–1045
34. Power JD, Barnes KA, Snyder AZ, Schlaggar BL, Petersen SE (2012) Spurious but systematic correlations in functional connectivity MRI networks arise from subject motion. *NeuroImage* 59:2142–2154
35. Regis J, Carron R, Park M (2010) Is radiosurgery a neuromodulation therapy?: A 2009 Fabrikant award lecture. *J Neuro-Oncol* 98:155–162
36. Rizzolatti G, Fogassi L, Gallese V (2002) Motor and cognitive functions of the ventral premotor cortex. *Curr Opin Neurobiol* 12:149–154
37. Saint-Cyr JA, Ungerleider LG, Desimone R (1990) Organization of visual cortical inputs to the striatum and subsequent outputs to the pallido-nigral complex in the monkey. *J Comp Neurol* 298:129–156
38. Schmidt R, Freidl W, Fazekas F, Reinhart B, Grieshofer P, Koch M, Eber B, Schumacher M, Polmin K, Lechner H (1994) The Mattis Dementia Rating Scale: normative data from 1,001 healthy volunteers. *Neurology* 44:964–966
39. Tardif E, Richer L, Bergeron A, Lepore F, Guillemot JP (1997) Spatial resolution and contrast sensitivity of single neurons in area 19 of split-chiasm cats: a comparison with primary visual cortex. *Eur J Neurosci* 9:1929–1939
40. Tuleasca C, Pralong E, Najdenovska E, Cuadra MB, Marques JRF, Vingerhoets F, Regis J, Bloch J, Levivier M (2017) Deep brain stimulation after previous gamma knife thalamotomy of the Vim for essential tremor is feasible! Clinical, electrophysiological and radiological findings. *Acta Neurochir* 159:1371–1373
41. Tuleasca C, Witjas T, Najdenovska E, Verger A, Girard N, Champoudry J, Thiran JP, Van de Ville D, Cuadra MB, Levivier M, Guedj E, Regis J (2017) Assessing the clinical outcome of Vim radiosurgery with voxel-based morphometry: visual areas are linked with tremor arrest! *Acta Neurochir* 159:2139–2144
42. Tuleasca C, Witjas T, Van de Ville D, Najdenovska E, Verger A, Girard N, Champoudry J, Thiran JP, Cuadra MB, Levivier M, Guedj E, Regis J (2017) Right Brodmann area 18 predicts tremor arrest after Vim radiosurgery: a voxel-based morphometry study. *Acta Neurochir*. <https://doi.org/10.1007/s00701-017-3391-x>
43. Witjas T, Carron R, Azulay JP, Regis J (2013) Gammaknife thalamotomy for intractable tremors: clinical outcome and correlations with neuroimaging features. *MDS 17th International Congress of Parkinson's Disease and Movement Disorders*, vol 28, p 1247
44. Witjas T, Carron R, Krack P, Eusebio A, Vaugoyeau M, Hariz M, Azulay JP, Regis J (2015) A prospective single-blind study of gamma knife thalamotomy for tremor. *Neurology* 85:1562–1568
45. Zeki S (1993) The visual association cortex. *Curr Opin Neurobiol* 3:155–159